RSC Advances

This is an *Accepted Manuscript*, which has been through the Royal Society of Chemistry peer review process and has been accepted for publication.

Accepted Manuscripts are published online shortly after acceptance, before technical editing, formatting and proof reading. Using this free service, authors can make their results available to the community, in citable form, before we publish the edited article. This *Accepted Manuscript* will be replaced by the edited, formatted and paginated article as soon as this is available.

You can find more information about *Accepted Manuscripts* in the Information for Authors.

Please note that technical editing may introduce minor changes to the text and/or graphics, which may alter content. The journal's standard Terms & Conditions and the Ethical guidelines still apply. In no event shall the Royal Society of Chemistry be held responsible for any errors or omissions in this *Accepted Manuscript* or any consequences arising from the use of any information it contains.

ROYAL SOCIETY OF CHEMISTRY

www.rsc.org/advances

Synthesis of chitosan-gelatin molecularly imprinted membranes for extraction of L-tyrosine

1. Introduction

Molecular imprinting is a technique for creating recognition sites for a specific analyte in a synthetic polymer [1-3]. Three steps are mainly implemented in synthesis of molecular imprinted polymers: (Ⅰ) functionalization of polymerizable monomer in order to interact with the template target specie, (Ⅱ) polymerization of the monomer-template complex in presence of suitable cross-linker and (Ⅲ) removal of the template molecules from the cross-linked matrix leaving specific recognition cavities, which are able to specifically rebind with the template target molecule in presence of other interfering species [4]. This imprinting process is therefore seen as a way to produce a range of materials with biomimetic recognition properties, with applications in separation [5-9], adsorption [10, 11], sensing [12-17], catalysis [18-25], drug delivery [26-31], etc. Currently, the molecularly imprinted membranes are mostly formed in an organic solvent, but the separation system of the membranes is soluble. With the focus of research shifted from the molecularly imprinted membrane lipophilic to hydrophilic organic small molecule compound, the molecular recognition system of water soluble will get more attention[32].

Chitosan is an N-deacetylated derivative of chitin, a cationic polysaccharide composed of b-D-glucosamine and N-acetyl-b-D-glucosamine residues with a 1,4 linkage. Due to its excellent biocompatibility, chitosan has been widely used in biomedical applications [33]. Chitosan is readily processible into films, beads and sponges from aqueous acid solution. A wet phase-inversion (immersion precipitation induced phase-inversion) method is a suitable technique to prepare macroporous gels with the desired morphology and pore size [34, 35].Several methods have been used to modify chitosan either physically [36] or chemically [37]; these modifications were proposed in order to improve pore size, mechanical strength, chemical stability, hydrophilicity and also biocompatibility. Nonetheless, few studies have been reported on the preparation of MIMs with chitosan and gelatin and no study has been reported

RSC Advances Accepted Manuscript

about the controlled release of drugs by nano-spherical magnetic MIMs. Hence, MIMs should be suitable as an ideal polymer material for wider applications.

The present work proposes a simple and efficient method for the preparation of MIMs to imprint L-tyrosine. L-tyrosine, CS-GEL and sulfuric acid as a template molecule, a functional monomer and a cross-linker, respectively, were copolymerized to form MIMs. And the structure of the chitosan-gelatin membranes was characterized by FTIR, X-ray diffraction and SEM. The special selective recognition capacity and permeability of MIMs was evaluated in aqueous solution.

2. Experimental details

2.1. Materials

Chitosan (CS, deacetylation degree of 90%) and gelatin were purchased from Yuhuan Factory, China. Polyethylene glycol (PEG) and L-tyrosine (L-try) were purchased from Tianjin chemical reagent co., LTD, China. All commercially solvents and reagents were used without further purification. All other chemicals were of analytical grade.

2.2. Preparation of molecular imprinted membrane (MIM)

Chitosan solution 3% (w/w) (prepared by adding chitosan into 2% (v/v) acetic acid solution) and polyethylene glycol (PEG) solution 6%(w/w) (prepared in aqueous solution at 60℃ ± 0.5℃) were dissolved by the ratio of 3:2 (w/w), Then polyethylene glycol (PEG, 3%, w/w) and a certain amount of L-tyrosine (Ltry) were added under vigorous stirring at 60℃ ± 0.5℃ for one hour. After eliminating the bubbles at 60℃ ± 0.5℃ for ten hours, 10mL solution was spread over the bottom of petri dishes(100mm diameter) or polycarbonate rectangular templates(300mm length × 150mm width) depending on the specific successive analysis. Final membranes were obtained and dried in a vacuum oven at 60 ± 0.5℃ for 10 h. And MIMs were sufficiently washed by sulfuric acid solution (0.1 mol/L) or glutaraldehyde solution for several times to extract the template molecules until the eluent was free from L-tyrosine as detected by UV-vis spectrometry (at 235 nm). The obtained membranes were finally rinsed with ethanol to remove the remaining acetic acid and dried in the

RSC Advances Accepted Manuscript

vacuum desiccator for 24 h before use.

For a comparison, non-molecularly imprinted polymers (CSG-NIMs), non-polyethylene glycol membranes (NPEG-MIMs) , and non-gelatin membranes (CS-MIMs) were prepared in the absence of L-tyrosine and PEG during the polymerization process and treated in the identical manner.

2.3 Swelling behaviour

To evaluate the water sorption resistance of the membranes, square piece of dry samples were weighed (W_i) and then immersed in distilled water at 30℃ with shaking (100 rmp) for up to 24h. Swollen membranes were removed from water periodically, blotted dry, and weighed (W_f) to track sportion kinetics. The swelling rate (SR) was determined as described by others[38] .

$$SR(\%)=[(W_f - W_i) / W_i]\times 100\% \quad (1)$$

2.4 Selectivity permeation experiments of membranes

Three kinds of mebranes (MIMs, NIMs and NP-MIMs) were fixed in the middle of the permeability pools (made in laboratory by myself, Figure 1) with the same area. Left of the permeability pools was added L-tyrosine solution 500ug/mL of sodium hydroxide solution (NaOH, 0.1mol/L), and right was added the same volume of sodium hydroxide solution (NaOH, 0.1mol/L). A certain volume solution (taken from the right permeability pools every 30 min) was detected the concentration of L-tyrosine by UV-vis, and the concentration of L-tyrosine at each moment of the experiment was calculated, according to the standard curve: A=0.00518+0.0359C.

2.5 Characterization

Fourier transform infrared spectroscopy (FT-IR)

All FTIR spectroscopic measurements were performed on a Bruker IFS 66/S (Germany). The sample powders were dried and mixed with KBr and pressed into a plate for measurement.

Ultraviolet–visible spectrum (UV–vis).

The concentrations of L-tyrosine in the solution were detected on a UV- 2401-PC

RSC Advances Accepted Manuscript

spectrometer (lambda 235 nm, Perkin Elmer Instrument, USA).

Scanning electron microscopy analysis (SEM)

Strips of dry film (10mm wide × 30mm long) were immersed in 30mL aliquots of 80wt.% ethanol water solution, with several changes. Then 80% ethanol was decanted and replaced with several changes of absolute ethanol. Next, strips were removed from absolute ethanol, quickly blotted dry and immersed in liquid Nitrogen for 5min. The frozen strips were cross fractured manually using cold tweezers and the fractured pieces were thawed in absolute ethanol. Finally, the fragments were critical point dried from liquid CO_2, and the dried fragments were glued to specimen stubs with Duco cement, sputter-coated with a thin layer of gold and examined with a Quanta 200 FEG scanning electron microscope, operated in the high vacuum, secondary electron imaging mode.

X-ray powder diffraction (XRD).

The structure of the membranes samples was characterized by XRD (Philips, Holland). The x-ray diffraction patterns were taken from 10◦ to 60◦ (2θ value) using Cu Kα radiation with an intensity ratio (α_1/α_2) = 0.5 and wavelengths of 1.544 39 and 1.540 56 Å, respectively.

3. Results and Discussion

3.1. Characterization of MIMs

3.1.1. Rationale of MIMs preparation

Control for space configuration, which is beneficial to imprinting molecule polymer network steadily combination of imprinting molecules around, in order to improve the selectivity of MIM membrane recognition function, performed assembly formed by the compound by crosslinking agent, the imprinting structure is fixed, after removal of imprinting molecule, and cavities are left in the CSG network which are high matched in size and shape with the template molecule.

Anyhow, binding is always significantly lower than that obtained with L-tyrosine under the various conditions tested. In L-tyrosine, indeed, benzene ring plays an

RSC Advances Accepted Manuscript

important role in the formation of the binding sites because of its interaction with the functional monomer (Figure 2), which is beneficial to imprint molecule polymer network steadily combination of imprinting molecules around. In order to improve the selectivity of MIMs recognition function, the imprinting structure (formed by crosslinker) was fixed after removing imprinting molecules, and imprinting molecules were matched in size and shape in MIMs network. This was one of the most important factors which lead to the selective interaction between the polymeric network and L-tyrosine.

3.1.2 FT IR analysis

Figure 3 gives the FTIR spectra of CS, Gelatin and CSG-MIMs. The absorption peaks at 3450cm^{-1} can be assigned to the N-H stretching of chitosan, at 1600cm^{-1} to the O-H stretching of chitosan, and at 2920 and 2881 cm^{-1} to the C-H stretching of chitosan. The absorption peaks at amide I band (1637 cm^{-1}) and the amide II band were very weak, which mainly because of the higher degree of deacetylation (90%) of chitosan. The absorption peaks at 1663 cm^{-1}, 1546 cm^{-1} and 1236 cm^{-1} can be assigned to the N-H bending vibrations of the amide Ⅰ, Ⅱ and Ⅲ band in curve GEL .[39] After polymerization, the vibrational band corresponding to primary amino groups at 1600cm^{-1} disappeared, while prominent bands at 1654 cm^{-1} was observed, which may be caused by the amidation reaction of amino and carboxyl . In addition, absorption peaks at 3500-3000 cm^{-1} became broader, which was caused by the hydrogen bonds. The absorption peaks were red shifted from 1637 cm^{-1} to 1628 cm^{-1} in C=O, and from 1063 cm^{-1} to 1058 cm^{-1} in C-O-C in the curve of CSG.

3.1.3 UV-vis analysis

Figure 4 (A) gives the Ultraviolet absorption spectra of L-tyrosine, eluent and CSG membrane in curve a, b, and c. The characteristic absorption peaks at 235nm can be assigned to benzene ring of L-tyrosine molecules (in curve a). After eluted, the absorption peaks in eluent (in curve b) became weaker than the L-tyrosine curve (in curve a), and the absorption peaks at 235nm disappeared in CSG (in curve c). Perfect activities (matching and imprinting molecule of L-tyrosine) were left in CSG membranes with the sulfuric acid as crosslinker by L-tyrosine molecule washed out.

RSC Advances Accepted Manuscript

Figure 4 (B) gives the effect of the ratio of CSG and molecular imprinting on binding sites. With the increasing of the amount of CSG, the UV absorption peaks of L-tyrosine became reduced. This was because that the binding sites of template molecules and CSG were increased and lead to the absorption peaks of L-tyrosine dissolved in solution decreased.

3.1.4 SEM analysis

The morphological structure of CSG-NIMs and CSG-MIMs were detected by SEM as shown in Figure 5. The structure of CSG-NIMs was dense without molecular imprinting (in Figure 5-A), and there was no any holes left on the surface of the polymer CSG. When template molecule was added into the system, the diffusion speed of solvent was increased with reducing the viscosity of system and the template molecule were embedded in the network structure of the polymer CSG. After washed the molecule off the obtained polymer by simple solvent, compared with CSG-NIMs , the binding sites was formed in CSG-MIMs which were complementary in size, shape and functional group to the template molecule and the diameter of the cavity was about 500nm (in Figure 5-B). Therefore, the obtained CSG-MIMs have special binding capacity, preconceived selectivity to template molecules.

3.1.5 XRD analysis

The X-ray diffraction patterns of membrane samples including chitosan membrane, gelatin membrane and chitosan-gelatin membrane are displayed in Figure 6.

The diffractogram of chitosan film presented in Figure 6 (a) shows the crystalline peaks (2θ) at 15.3 and 20.2°, which are typical fingerprint for chitosan film and very similar to the work of Wan, Creber, Preppley, and Bui[40]. From previous report [41], the small peak at approximately 15° (2θ) was attributed to the anhydrous crystal of chitosan whereas the diffraction peak at around 21-22° (2θ) was observed in chitosan film prepared from dissolving chitosan in acetic acid solution[42]. In this study, however, the intensity of the crystal peak at about 21.18 (2θ) is very low, indicating low crystallinity. It is noted that the degree of deacetylation has obviously affected crystallinity of chitosan film. According to the previous research (Wan et al.), it was observed that the crystallinity of the chitosan film increased gradually with increasing

RSC Advances Accepted Manuscript

degree of deacetylation ranging from 70 to 90%. This may be attributed to the fact that chains of chitosan with higher degree of deacetylation are more compact leading to facilitate the hydrogen bonding formation and in turn crystallinity formation in the film. Furthermore, higher degree of deacetylation chitosan contains more glucosamine groups, which also facilitate the hydrogen-bonding formation. On the contrary, lower degree of deacetylation chitosan has more acetyl groups, which hinder the chitosan chain packing due to their rigidity and steric effect. Therefore, the chitosan films prepared from the high degree of deacetylation chitosan contain a large crystalline region. It is quite rare that the production of chitosan with 100% degree of deacetylation is achievable. Therefore, commercial chitosan with various degree of deacetylation in the range of 75-85% is commonly found.

The pattern of gelatin, as shown in Figure 6(b), had a diffraction peak at11.1° (2θ) and 20.5° (2θ) [43]. If chitosan and gelatin have very low compatibility, each polymer would have its own crystal region in the blends, so X-ray diffraction patterns are expressed as simply mixed patterns of chitosan and gelatin with the same ratio as those for blending. However, the intensity of diffraction peak at 11.1° (2θ) and 18.4° (2θ) of composite film increased compared with that of chitosan film, and a new peak appeared at 16.5° (2θ) in Figure 6(c).

When a chitosan-gelatin polyelectrolyte complex forms, amino groups in chitosan form hydrogen bonding with carboxyl groups in gelatin. This formation breaks the hydrogen bonding between amino groups and hydroxyl groups in chitosan and then results in an amorphous structure of the polyelectrolyte complex. Similar explanations for the deformation of crystal structure have been discussed in several references [44, 45]. The decreased crystallinity of composite films also implies that the hydrogen bonding between gelatin and chitosan leads to their good compatibility.

3.2 Effect of the type of crosslinker on the structure properties of the membrane

Glutaraldehyde and sulfuric acid were selected as crosslinking agent, respectively. Glutaraldehyde as crosslinking agent (in Formular 2), it was easy to form a covalent bond with high degree of crosslinking polymer between glutaraldehyde and $-NH_2$ of chitosan, and cause difficulties to elute the imprinting molecule L-tyrosine

RSC Advances Accepted Manuscript

and to recycle L-tyrosine again. At the same time, the high crosslinking degree will reduces the accessibility of imprinted loci and the mass transfer rate, so as to restrict the practical application of molecular imprinting technique. In addition, molecularly imprinted membrane using glutaraldehyde as crosslinking agent was easily broken and difficultly filmed. So glutaraldehyde crosslinking agent was not the best to form membrane.

However, chitosan-gelatin membrane crosslinked by H_2SO_4 (in Formular 3) was easy to form ionic bond between SO_4^{2-} and - NH_3^+ (by the protonation of -NH_2 in chitosan), and it was conducive to the stability of the membrane structure through ions.[46] Therefore, crosslinking agent of H_2SO_4 was the better to form membrane in practical applications.

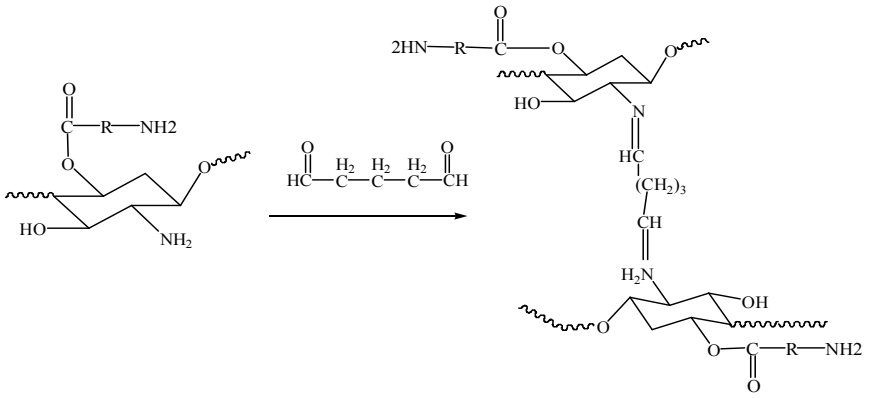

(2)

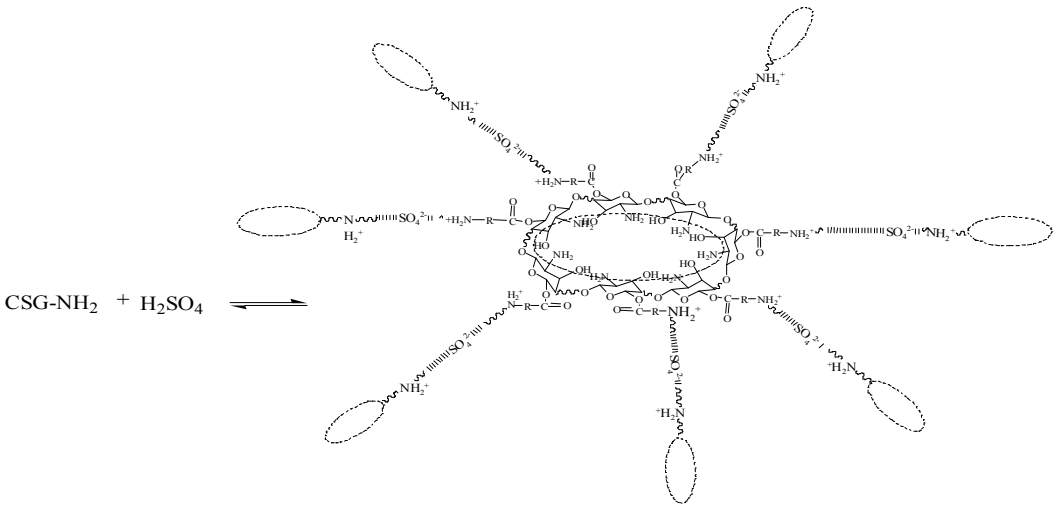

(3)

3.3 Effect of imprinting molecular content on permeability of membrane

RSC Advances Accepted Manuscript

Figure 7 was the effect of imprinting molecule content on the permeating quantity. The content of imprinting molecular is one of the important parameters that affect the separation performance of molecularly imprinted membrane. The lower of the content of molecular imprinting, the less identify points were formed in molecularly imprinted membrane, and reducing the ability to identify. When the content was too high, identify points increased, but it was easy to form structural defects. When $m_{CSG} : m_{L\text{-tyrosine}} = 20:1$, dry membrane permeation was the largest, and the membrane was the best.

3.4 The swelling properties of molecular imprinted membranes

With static swelling method, the quality of the molecularly imprinted membrane was weighed after immersed in distilled water for 72 h by mass and density variation ratio. According to Formula 1, the swelling rate of molecularly imprinted membrane was 9.55% (in Table 1). Chitosan and gelatin, respectively, has a very strong hydrophilicity, but after cross-linked into a network structure, the swelling properties of chitosan-gelatin membrane in aqueous changed a little, indicating that the internal structure of the membrane did not change greatly, and the membrane could be stable separation performance and be used for a long-term.

3.5 The permeability properties of molecular imprinted membranes

Figure 8 showed the permeation curves of the mixture solutes through a (CSG-MIM), b(NPEG-MIM), c(CSG-NIM), and d(CS-MIM). As shown by Figure 8, at the same time, the permeability of the L-tyrosine through molecular imprinted membrane was much greater than b, c, and d. When the permeation time was 10 h, the permeability rate of L-tyrosine (a, b, c, and d) was 13.42%, 6.31%, 5.22%, and 9.35%, respectively. And the permeability rate of 5 - sulfosalicylic acid (5-SA) was more or less to a, b and c. This was because that the specific recognition capacity of the polymer was achieved by forming a complex between the template molecule L-tyrosine and the chitosan-gelatin membrane in the molecularly imprinted membranes (MIMs). Removal of the template molecule L-tyrosine from the MIMs revealed binding sites that were complementary in size, shape and functional group to the template molecule L-tyrosine. Therefore, the obtained MIMs have special

RSC Advances Accepted Manuscript

selectivity to template molecules L-tyrosine. As to NPEG-MIM and CSG-NIM, because there were no binding sites left, the irregular cavities were easily clogged by molecules, resulting in template molecules L-tyrosine by generally low permeability rate [47]. The studies of membranes penetration experiment showed that molecularly imprinted membrane can effectively separated L-tyrosine from other substances in the water phase and the permeability rate of L-tyrosine was 13.42%. The permeability rate of L-tyrosine of CSG-MIM (13.42%) was better than that of CS-MIM (9.35%), because, after crosslinked between chitosan and gelatin, it was easier to form a space network structure with the template molecules embedded in the mesh structure. After the template molecules eluted, many binding sites were left in the polymer. Therefore, CSG-MIMs have more broad prospects for development in the field of penetration.

4 Conclution

The present study describes the development of molecularly imprinted polymers for special recognition and permeability of L-tyrosine. Chitosan and gelatin were used to prepare MIMs. The MIMs exhibited good special binding and selectivity capacities to the template molecule. This study indicated that the prepared MIMs possess the combined properties of selective recognition and permeability.

The combination of these factors suggests that molecularly imprinted polymers will be both better defined and will have properties of real value in the biomedical field, leading to a promising future for these materials as separation devices.

ACKNOWLEDGEMENTS

We are very much grateful to Dr. Qi Lian for providing necessary facility to conduct the research work. The authors acknowledge the financial support from Education Department of Hebei Province(Q2012056) and Technology Bureau of Qinhuangdao (2012021A127).

RSC Advances Accepted Manuscript

REFERENCES

[1] G. Wulff. *Angew Chem Int Engl* 1995; 34: 1812-1832.

[2] G Vlatakis, L. I. Andersson, R M ueller, K. Mosbach. *Nature* 1993, 361: 645-7.

[3] K.J. Shea. *Trends Polym Sci*, 1994;2:166–73.

[4] S. J. Ahmadi, O. Noori-Kalkhoran, S. Shirvani-Arania. *J. Hazard. Mater.* 2010, 175: 193-197

[5] M.J. Whitcombe, E. N. Vulfson. Adv Mater, 2001, 13: 467-478.

[6] L. I. Andersson. *J Chromatogr B,* 2000, 739: 163–73.

[7] X. Chen, Z. H. Zhang, X. Yang, Y. N. Liu, J. X. Li, M. J. Peng, S. Z. Yao. *J Sep Sci* , 2012, 35: 2414-2421.

[8] P. Lulinski, D. Maciejewska. *J Sep Sci,* 2012, 35: 1050-1057.

[9] W.J. Cheong, S.H. Yang, F. Ali. *J Sep Sci*, 2013, 36: 609-628.

[10] S. J. Li, Y. Ge, S.A. Piletsky, A.P.F. Turner. *Adv Funct Mater*, 2011, 21: 3344-3349.

[11] Z.H. Meng, Q.Y. Zhang, M. Xue, D. Wang, A. Wang. *Propel Explos Pyrot*, 2012, 37: 100-106.

[12] L. Ye, I. Surugiu, K. Haupt. *Anal Chem*, 2002, 74: 959-964.

[13] D. Lakshmi, A. Bossi, M.J. Whitcombe, I .Chianella, S.A. Fowler, S. Sub-rahmanyam, E.V. Piletska, S.A. Piletsky. *AnalChem*, 2009, 81: 3576-3584.

[14] R. Schirhagl, D. Podlipna, P.A. Lieberzeit, F.L. Dickert. *Chem Commun*, 2010, 46: 3128-3130.

[15] R.N. Liang, D.A. Song, R.M. Zhang, W. Qin. *Angew Chem Int Ed* , 2010, 49: 2556-2559.

[16] F. Liu, S.Y. Huang, F. Xue, Y.F. Wang, Z.H. Meng, M. Xue. *Biosens Bioelectron*, 2012, 32: 273-277.

[17] Y. Fuchs, O. Soppera, A.G. Mayes, K. Haupt. *Adv Mater*, 2013, 25: 566-570.

[18] J.Q. Liu, G. Wulff. *J AmChem Soc,* 2008, 130: 8044-8054.

[19] J.Q. Liu, G. Wulff. *Angew Chem Int Ed*, 2004, 43: 1287-1290.

[20] J.Q. Liu, G. Wulff. *J Am Chem Soc*, 2004, 126: 7452-7453.

RSC Advances Accepted Manuscript

[21] G. Wulff. *Chem Rev,* 2002, 102: 1-27.

[22] J. Matsui, I.A. Nicholls, I. Karube, K. Mosbach. *J Org Chem*, 1996, 61: 5414-5417.

[23] J. Hedin-Dahlström, J.P. Rosengren-Holmberg, S. Legrand, S. Wikman, I.A. Nicholls. *J Org Chem*, 2006, 71: 4845-4853.

[24] N. Kirsch, J. Hedin-Dahlström, H. Henschel, M.J. Whitcombe, S. Wikman, I.A. Nicholls. *J Mol Catal B*, 2009, 58: 110-117.

[25] S.J. Li, Y. Ge, A.P.F. Turner. *Adv Funct Mater*, 2011, 21: 1194-1200.

[26] M.E. Byrne, J.Z. Hilt, N.A. Peppas. *J BiomedMater Res A*, 2008, 84: 137-147.

[27] F. Puoci, F. Iemma, N. Picci. *Curr Drug Deliv*, 2008, 5: 85-96.

[28] G. Cirillo, F. Iemma, F. Puoci, O.I. Parisi, M. Curcio, U.G. Spizzirri, N.Picci. *J Drug Target*, 2009, 17: 72-77.

[29] S.J. Li, A. Tiwari, Y. Ge, D. Fei. *Adv Mater Lett*, 2010, 1: 4-10.

[30] F. Puoci, G. Cirillo, M. Curcio, O.I. Parisi, F. Iemma, N. Picci. *Expert Opin Drug Deliv*, 2011, 8: 1379-1393.

[31] K. Rostamizadeh, M. Vahedpour, S. Bozorgi. *Int J Pharm*, 2012, 424: 67-75.

[32] X.M. Chen, X.Q. Cao, Z.Y. Yu. *Polym Mater Sci Eng*, 2012, 28(8): 163-166

[33] X. F. Zheng, Q. Lian, H. Yang. *Asian J Chem*, 2013, 25(4): 2121-2124.

[34] F. L.Mi, S. S. Shyu, C. T. Chen, J. Y. Lai. *Polym*, 2002, 43, 757-765.

[35] W. S.W. Ngah, C. S. Endud, R. Mayanar. *React Funct Polym*, 2002, 50, 181-190.

[36] X. Z. Shu, K. J. Zhu. *J Microencapsul*, 2001, 18, 237-245.

[37] X. F. Zheng, Q. Lian, S. T. Song., Asian J Chem, 2013, 25(10): 5363-5366.

[38] D. Myung, D.Waters, M. Wiseman, P.E. Duhamel, J. Noolandi, C.N. Ta. *Polym. Adv. Technol.,* 2008, 19, 647.

[39] C. B. Xiao, Y. S. Lu, S. J. Cao. *J Appl Polym Sci*, 2001, 79: 1596-1602

[40] Y.Wan, K.A.M. Creber, B. Preppley, V.T. Bui. *Polymer*, 2003, 44: 1057-1065

[41] P.C. Srinivasa, M.N. Ramesh, K.R. Kumar, R.N. Tharanathan. *J Food Eng*, 2004, 63: 79-85.

[42] G. C. Ritthidej, T. Phaechamud, T. Koizumi. *Int J Pharmaceut*, 2002, 232: 11-22.

RSC Advances Accepted Manuscript

[43] H. Y. Yan, K.H. Row. *Sep Sci Techno1*. 2006, 41(9): l84l-1855.

[44] Y.M. Lee, S.Y. Nam, J.H. Kim. *Polym Bull*, 1992, 29: 423-428.

[45] H.J. Kim, M.Y. Lee. *Polymer*, 1993, 34: 1952-1957.

[46] Z. Cui, Y. Xiang, T. Zhang. Acta Chimica Sinaca, 2007, 65(17): 1902-1906.

[47] J.P. Lai, C.Y. Lu, X.W. He. Chemical Journal of Chinese Universities, 2003, 24(7): 1175-1179.

RSC Advances Accepted Manuscript

Figure Captions

Figure1 Schematic diagram of imprinted membrane

Figure 2. Schematic diagram of the formation process of L-tyrosine imprinted CSG membrane

Figure 3 FT IR spectra of CS, Gelatine and CSG-MIMs (m_{CS}：m_{GEL}=20：1, sulfuric acid as crosslinker，removed imprinted molecule)

Figure 4 UV-vis absorbance spectra of L-tyrosine

Figure 5 SEM images of imprinted membranes : A) NPEG-MIM; B) CSG-MIM

Figure 6 X-ray diffractograms of: (a) chitosan membrane, (b) gelatin membrane, (c)chitosan-gelatin membrane

Figure 7 Effect of imprinting molecule content on the permeating quantity(PQ)

Figure 8 Permeation curves of the mixture solutes through a (CSG-MIM, m_{CS}：m_{GEL} = 20: 1, H_2SO_4 as the crosslinker, the imprinted molecular had eluted), b(NPEG-MIM) and c(CSG-NIM)

Table 1 The swelling rate of the Molecularly imprinted membrane

RSC Advances Accepted Manuscript

RSC Advances Accepted Manuscript

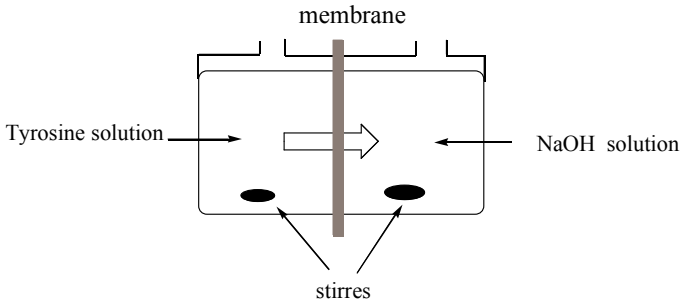

Figure1 Schematic diagram of imprinted membrane

RSC Advances Accepted Manuscript

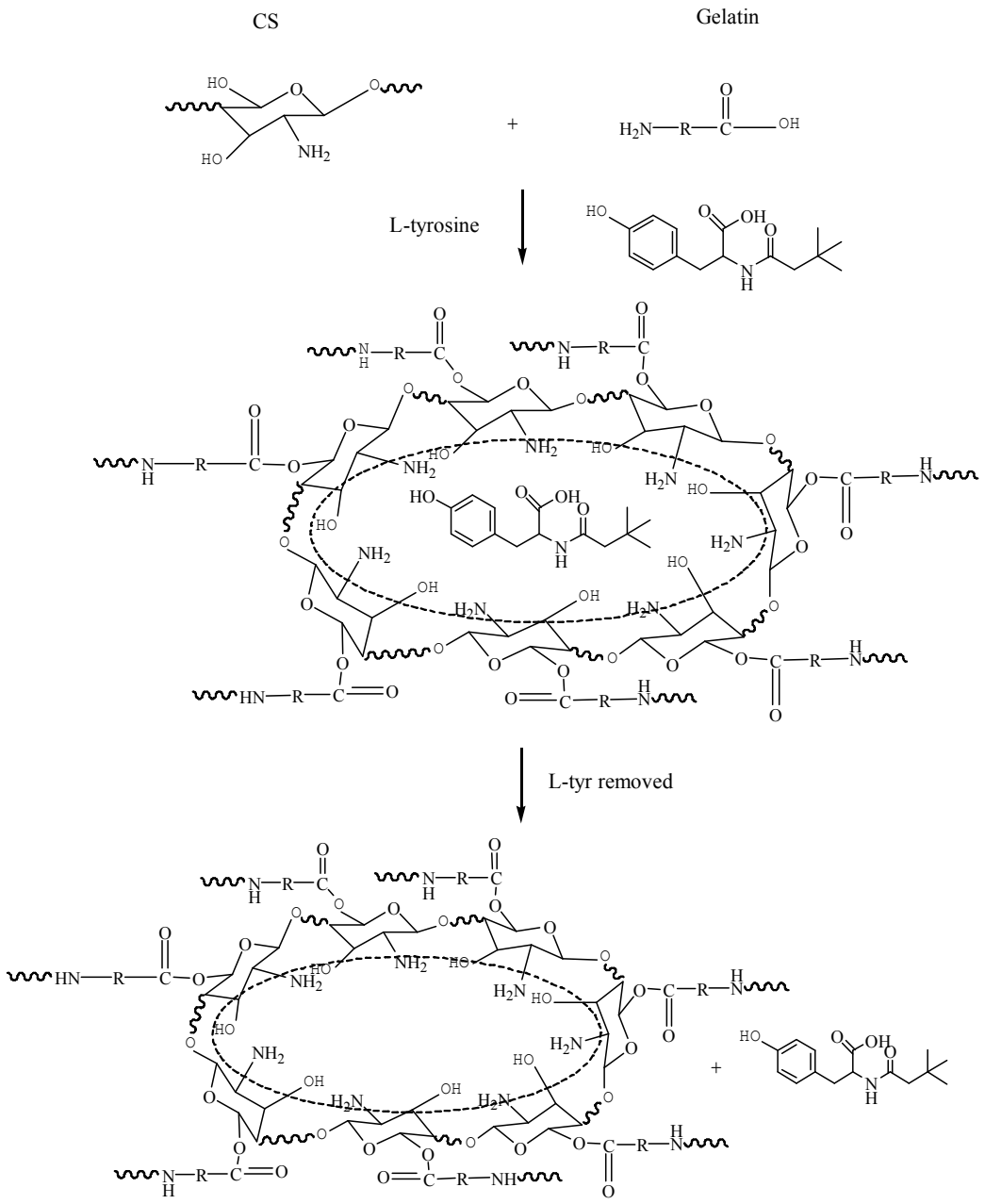

Figure 2. Schematic diagram of the formation process of L-tyrosine imprinted CSG membrane

RSC Advances Accepted Manuscript

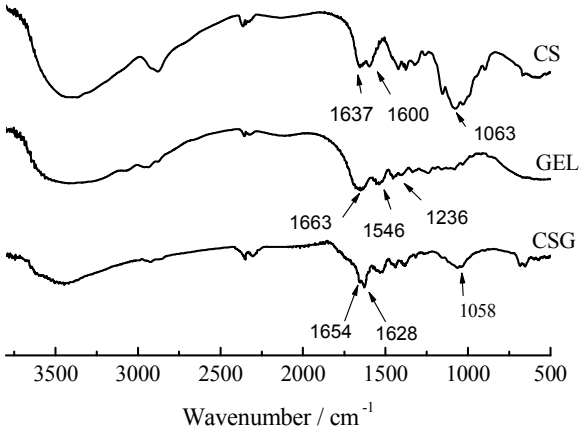

Figure 3 FT IR spectra of CS, Gelatine and CSG-MIMs (m_{CS}：m_{GEL}=20：1, sulfuric acid as crosslinker，removed imprinted molecule)

RSC Advances Accepted Manuscript

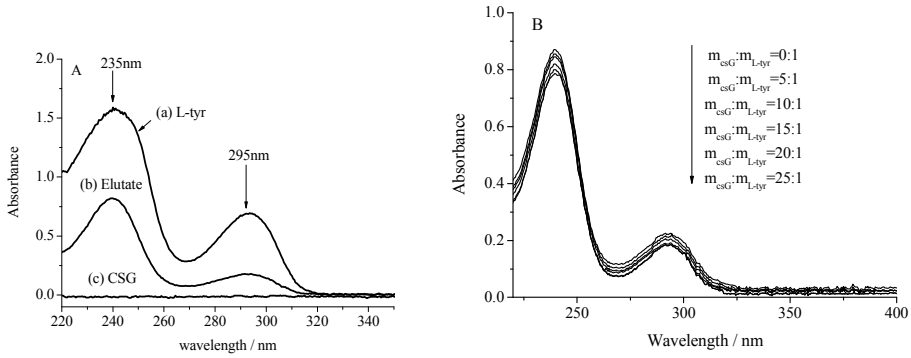

Figure 4 UV-vis absorbance spectra of L-tyrosine

RSC Advances Accepted Manuscript

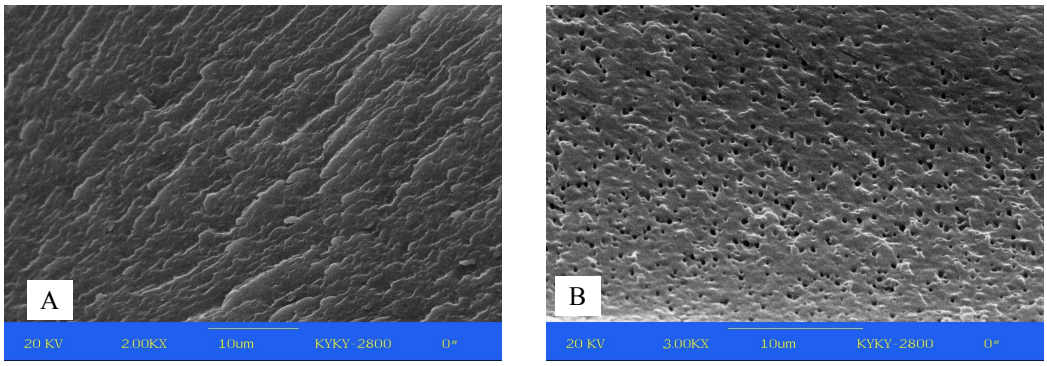

Figure 5 SEM images of imprinted membranes : A) CSG-NIM; B) CSG-MIM, molecular imprinting is washed off CSG-MIM

RSC Advances Accepted Manuscript

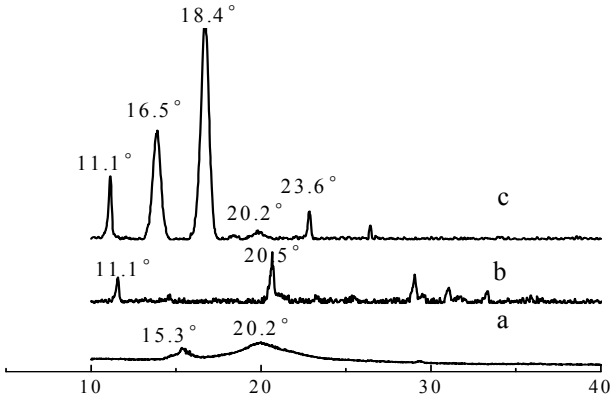

Figure 6 X-ray diffractograms of: (a) chitosan membrane, (b) gelatin membrane, (c)chitosan-gelatin membrane

RSC Advances Accepted Manuscript

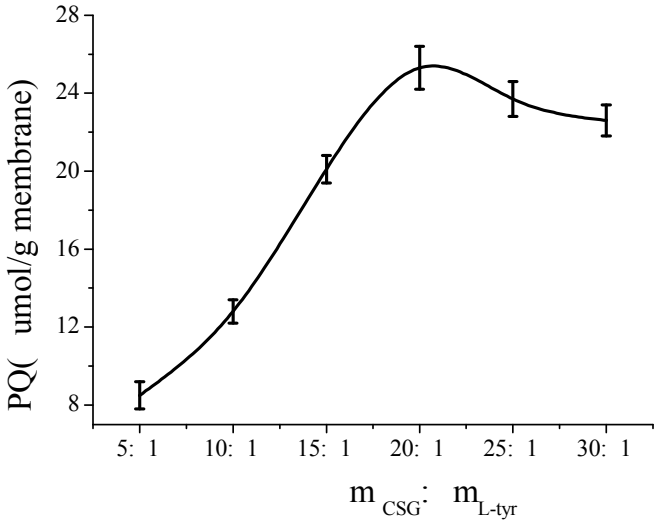

Figure 7 Effect of imprinting molecule content on the permeating quantity(PQ)

RSC Advances Accepted Manuscript

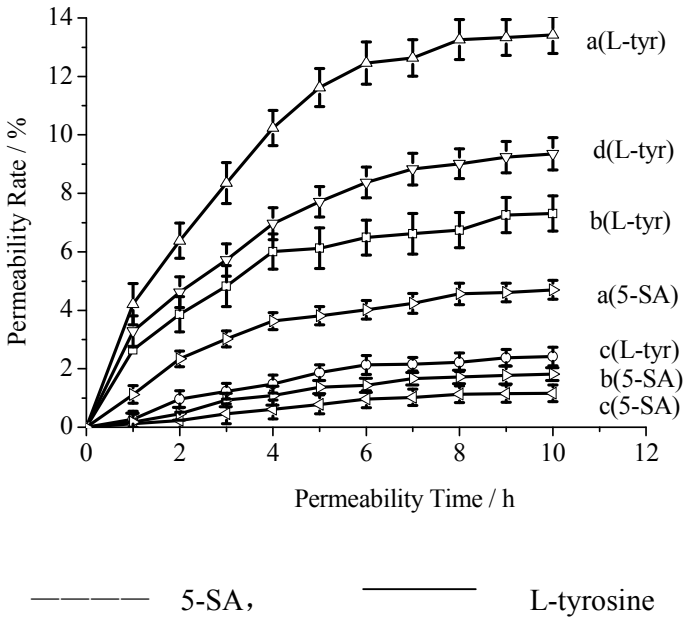

Figure 8 Permeation curves of the mixture solutes through a (CSG-MIM, m_{CS}：m_{GEL} = 20: 1, H_2SO_4 as the crosslinker, the imprinted molecular had eluted), b(NPEG-MIM), c(CSG-NIM) and d (CS-MIM).

RSC Advances Accepted Manuscript

Table 1 The swelling rate of the Molecularly imprinted membrane

Samples	1	2	3	4	5
m_d/g	1.0132	0.9879	1.1125	1.1625	1.0043
m_s/g	1.1121	1.0823	1.2132	1.2725	1.1038
SR/%	9.7612	9.5556	9.0517	9.4624	9.9074
Average/%			9.55		

RSC Advances Accepted Manuscript

Abstract

In this work, the chitosan-gelatine-L-tyrosine(CS-GEL-L-tyr) moleculary imprinted membranes (MIMs) was prepared in aqueous phase using CS and GEL as the functional polymers, L-tyrosine as an imprinting molecule, polyethylene glycol (PEG) as a porogen. Removal of the template molecule L-tyrosine from the MIMs revealed binding sites that were complementary in size, shape and functional group to the template molecule L-tyrosine, which were investigated using SEM, FTIR and XRD. The effect of various significant parameters such crosslinking agent, PEG concentration and imprinting molecular content were examined and the results indicated that the obtained MIMs have special selectivity to template molecules L-tyrosine, molecularly imprinted membrane can effectively separated L-tyrosine from other substances in the water phase and the permeability rate of L-tyrosine was 13.42%.

RSC Advances Accepted Manuscript

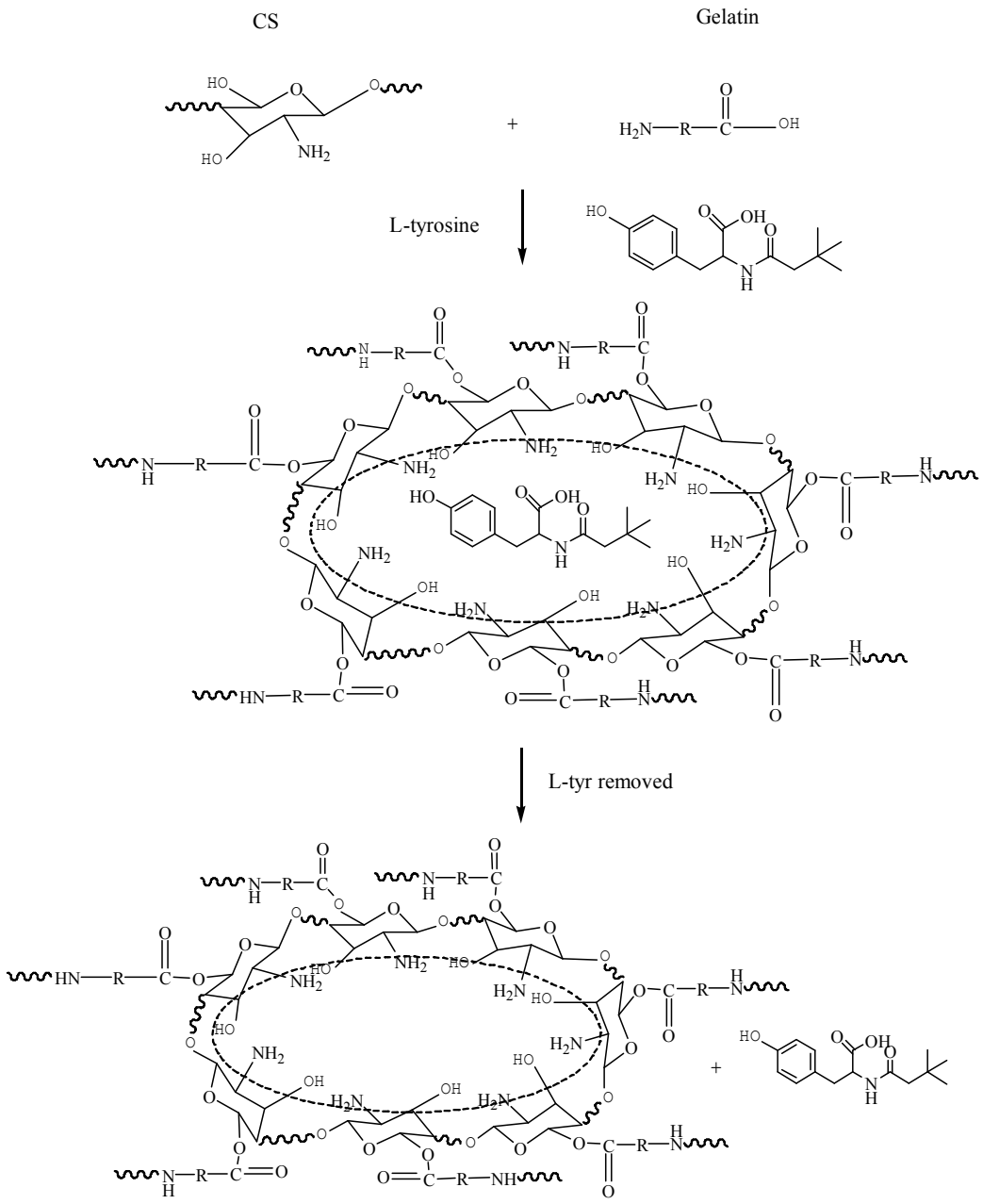

Figure 2. Schematic diagram of the formation process of L-tyrosine imprinted CSG membrane

RSC Advances Accepted Manuscript